



DEMETER plays a role in DNA demethylation and disease response in somatic tissues of Arabidopsis

Ulrike Schumann, Joanne M. Lee, Neil A. Smith, Chengcheng Zhong, Jian-Kang Zhu, Elizabeth S. Dennis, Anthony A. Millar & Ming-Bo Wang


To cite this article: Ulrike Schumann, Joanne M. Lee, Neil A. Smith, Chengcheng Zhong, Jian-Kang Zhu, Elizabeth S. Dennis, Anthony A. Millar & Ming-Bo Wang (2019): *DEMETER* plays a role in DNA demethylation and disease response in somatic tissues of Arabidopsis, Epigenetics, DOI: 10.1080/15592294.2019.1631113

To link to this article: <https://doi.org/10.1080/15592294.2019.1631113>

 View supplementary material 

 Accepted author version posted online: 12 Jun 2019.
Published online: 19 Jun 2019.

 Submit your article to this journal 

 Article views: 108

 View Crossmark data 

RESEARCH PAPER



DEMETER plays a role in DNA demethylation and disease response in somatic tissues of Arabidopsis

Ulrike Schumann^{ib}^{a*}†, Joanne M. Lee^{a*}‡, Neil A. Smith^a, Chengcheng Zhong^a, Jian-Kang Zhu^b, Elizabeth S. Dennis^a, Anthony A. Millar^c, and Ming-Bo Wang^a

^aCSIRO Agriculture and Food, Acton, Australia; ^bDepartment of Horticulture and Landscape Architecture, Purdue University, West Lafayette, IN, USA; ^cResearch School of Biology, Australian National University, Acton, Australia

ABSTRACT

DNA demethylases function in conjunction with DNA methyltransferases to modulate genomic DNA methylation levels in plants. The Arabidopsis genome contains four DNA demethylase genes, *DEMETER* (*DME*), *REPRESSOR OF SILENCING 1* (*ROS1*) also known as *DEMETER-LIKE 1* (*DML1*), *DML2*, and *DML3*. While *ROS1*, *DML2*, and *DML3* were shown to function in disease response in somatic tissues, *DME* has been thought to function only in reproductive tissues to maintain the maternal-specific expression pattern of a subset of imprinted genes. Here we used promoter:β-glucuronidase (*GUS*) fusion constructs to show that *DME* is constitutively expressed throughout the plant, and that *ROS1*, *DML2*, and *DML3* have tissue-specific expression patterns. Loss-of-function mutations in *DME* cause seed abortion and therefore viable *DME* mutants are not available for gene function analysis. We knocked down *DME* expression in a triple *ros1 dml2 dml3* (*rd*) mutant background using green tissue-specific expression of a hairpin RNA transgene (*RNAi*), generating a viable 'quadruple' demethylase mutant line. We show that this *rd* *DME* *RNAi* line has enhanced disease susceptibility to *Fusarium oxysporum* infection compared to the *rd* triple mutant. Furthermore, several defence-related genes, previously shown to be repressed in *rd*, were further repressed in the *rd* *DME* *RNAi* plants. DNA methylation analysis of two of these genes revealed increased differential promoter DNA methylation in *rd* *DME* *RNAi* plants compared to WT, beyond the difference observed in the parental *rd* plants. These results indicate that *DME* contributes to DNA demethylase activity and disease response in somatic tissues.

ARTICLE HISTORY

Received 4 March 2019
Revised 28 May 2019
Accepted 5 June 2019

KEYWORDS

DEMETER; DEMETER-LIKE; *ROS1*; *rd*; DNA-demethylation; *Fusarium*; *Arabidopsis thaliana*; Epigenetics

Introduction

DNA cytosine methylation is a major epigenetic mark in eukaryotes. In plants, the DNA methylation level in the genome is controlled by *de novo* DNA methylation, maintenance DNA methylation and DNA demethylation. *De novo* methylation is mediated by RNA-directed DNA methylation (RdDM), which can occur at all cytosine contexts, namely CG, CHG ('H' stands for A, C, T) and CHH sites. Methylation at symmetric CG and CHG sites can be maintained during DNA replication by METHYLTRANSFERASE 1 (*MET1*) and CHROMOMETHYLASE 3 (*CMT3*), respectively. CHH methylation at highly repetitive regions of the genome can be maintained by *CMT2*, but CHH methylation near genes cannot be maintained during DNA replication and depends on

continuous RdDM. DNA demethylation can occur passively during DNA replication when maintenance methylation is incomplete, or through the activity of the DNA glycosylase family of DNA demethylases. These DNA demethylases remove 5-methylcytosine and replace it with unmethylated cytosine through a base-excision-repair mechanism [1].


The Arabidopsis genome contains four DNA demethylase genes, *DEMETER* (*DME*), *REPRESSOR OF SILENCING 1* (*ROS1*) also known as *DEMETER-LIKE 1* (*DML1*), *DML2*, and *DML3* [1]. *DME* has been shown to play a major role in seed development by controlling the expression of specific imprinted maternal alleles, and mutation of the maternal copy of the *DME* gene leads to seed abortion [2,3]. *ROS1*, *DML2*, and *DML3* are thought to account for all

CONTACT Ming-Bo Wang  ming-bo.wang@csiro.au  CSIRO Agriculture and Food, Clunies Ross Street, Acton, ACT 2601, Australia

*These authors contributed equally to this work

†Present address: EMBL-Australia Collaborating Group, John Curtin School of Medical Research, Australian National University, Acton, ACT 2601, Australia

‡Present address: Plant Health Australia, Deakin, ACT 2600, Australia

 Supplemental data for this article can be accessed [here](#).

© 2019 Informa UK Limited, trading as Taylor & Francis Group

demethylase activities in somatic tissues. ROS1 is the dominant demethylase of the three and plays a role in maintaining the activity of transgenes and transposable elements in Arabidopsis by decreasing DNA methylation [1]. Both localized and genome-wide DNA methylation analyses have shown that DML2 and DML3 function redundantly with ROS1 to maintain low-level cytosine methylation at some loci [4,5]. DML2 and DML3 have also been shown to play a role in modulating the DNA methylation level of some heavily methylated loci in Arabidopsis [6]. In addition to maintaining genome methylation levels, the three DNA demethylase genes have recently been implicated in plant disease resistance in Arabidopsis. The single mutant *ros1*, and the triple mutant *ros1 dml2 dml3 (rdd)*, have been shown to display increased susceptibility to the bacterial pathogen *Pseudomonas syringae* [7] and the fungal pathogen *Fusarium oxysporum* [8], suggesting that these DNA demethylases play a role in plant defence responses by regulating plant defence-related genes.

The expression patterns of the four DNA demethylase genes have been investigated. Choi et al. [3] reported that *DME* is expressed specifically in the central cells of female gametophytes, but is undetectable in leaf tissues using RT-PCR. In contrast, Ortega-Gallisteo et al. [6] detected the constitutive expression of *DME* as well as *ROS1*, *DML2* and *DML3* across various plant tissues using RT-PCR. Further, they used promoter: β -glucuronidase (GUS) constructs to examine the expression pattern of *DML2* and *DML3*, and showed that both genes are strongly expressed in all tissues of Arabidopsis. Gong et al. [9] also used promoter:GUS reporter constructs to investigate the expression pattern of *ROS1*, and showed strong expression in all tissues of young Arabidopsis seedlings. *DME*, *ROS1* and *DML2* expression patterns are also represented in the Arabidopsis Gene Expression Visualization database (AtGenExpress [10]), which shows constitutive expression of *DME* but more variable expression levels of *ROS1* and *DML2* across different plant tissues (Supplementary Figure S1A). No *DML3* expression data were recorded as *DML3* was not represented on the Affymetrix ATH-1 array. However, *DML3* RNA sequencing data are available in the Transcriptome Variation Analysis database (TraVA [11]), which shows the localized expression of *DML3* in anthers only. In support of this, our previous microarray expression analysis [8] and

mRNA sequencing (unpublished) of 3-week-old whole Col-0 Arabidopsis seedlings detected the low-level expression of *DML3* along with the relatively high-level expression of *DME*, *ROS1* and *DML2* (Supplementary Figure S1B, S1C). This contradicts the reported constitutive expression pattern of *DML3* [6]. Thus, the expression patterns of the four demethylase genes require further examination, but it seems clear that *DME* has a widespread expression in both reproductive and vegetative tissues of Arabidopsis.

The observed *DME* expression pattern raised the possibility that *DME* not only functions in reproductive tissue but also contributes to DNA demethylase activity and related biological function in the whole plant. However, this has not been investigated, possibly because a loss-of-function mutation in *DME* results in seed abortion, and therefore double, triple, or quadruple demethylase mutants containing a *DME* mutation are not available for genomic and biological function studies. Indeed, genome-wide methylation and gene expression studies utilized either single DNA demethylase mutants or the triple demethylase mutant *rdd*. Both DNA methylation and gene expression changes in *rdd* are limited, with a relatively small number of loci affected by the mutations [4,12,13]. The functional analysis of the DNA demethylases in disease resistance has also been based on the use of the single *ros1* and triple *rdd* mutants [5,7,8].

The present study was aimed at examining the biological function of *DME* in somatic tissues. Using promoter:GUS fusion constructs, we confirmed the constitutive expression pattern of *DME* and revealed tissue-differential or tissue-specific expression patterns of *ROS1*, *DML2* and *DML3*. We knocked down the expression of *DME* in the *rdd* mutant background using green tissue-specific RNAi to generate a viable *rdd DME* RNAi line. We used this line to demonstrate that *DME* plays a role in *Fusarium* resistance, defence gene expression and DNA demethylation in vegetative Arabidopsis tissues.

Results

***DME*, *ROS1*, *DML2* and *DML3* promoters show distinct expression patterns**

The structures of the promoter:GUS fusion constructs are illustrated in Figure 1. The promoter

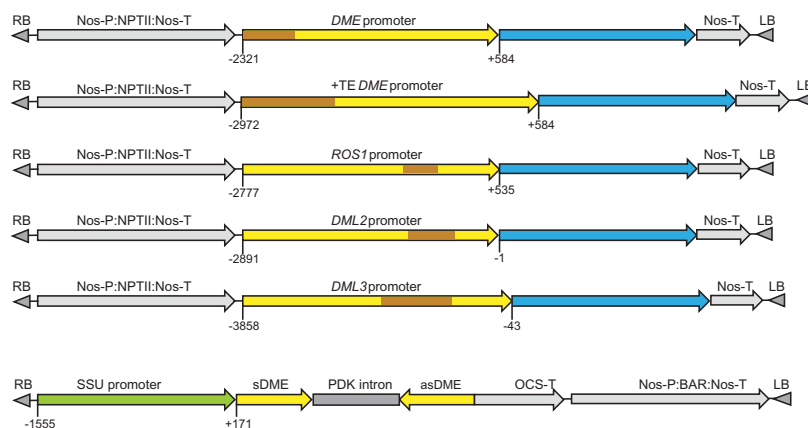


Figure 1. Schematic diagrams of the promoter:GUS fusion constructs and the *DME* hairpin RNA (hpDME) construct. Transposable element (TE) sequences are indicated in brown; blue regions indicate the GUS coding sequence. Numbers indicate the nucleotide position relative to the transcription start site (TSS).

fragments were amplified from the genomic region upstream of the translation start site ATG, with the size of 2.90 and 3.56 kb (*DME*; -2321 to $+584$ and -2972 to $+584$ relative to the transcription start site or TSS), 3.31 kb (*ROS1*; -2777 to $+535$), 2.89 kb (*DML2*; -2891 to -1), and 3.82 kb (*DML3*; -3858 to -43), respectively. These promoter fragments contain longer upstream sequences than the previously used ones for *DME* (-2282 to 1922 bp of the first exon) [3], *ROS1* (-1565 to -25 from first ATG or -1030 to $+510$ relative to TSS) [9], *DML2* (-2269 to $+15$ from first ATG or TSS) and *DML3* (-1300 to $+13$ from first ATG or -1145 to $+171$ relative to TSS) [6] promoters, respectively. Two versions of the *DME* promoter were tested; one included the full-length upstream transposable element (TE) sequence (*DME+TEp*) in case the TE plays a role in *DME* regulation, and the second (*DMEp*) contained part of the TE but excluding the upstream section that overlaps with the transcription start site of the adjacent gene. The *ROS1*, *DML2* and *DML3* promoter fragments also contained TE sequence that exists in the upstream genomic sequences of the respective genes (Figure 1). To avoid the potential enhancer effects by strong constitutive promoters such as the 35S promoter [14], the promoter:GUS expression cassettes were cloned into the plant expression vector pBI101, where the selective marker gene *NPTII* is driven by the relatively weak nopaline synthase promoter (Nos-P), which is located distal to the inserted endogenous gene promoters (Figure 1).

Transgenic lines of the Col-0 ecotype were obtained, self-fertilized until the fourth generation, and then analysed for GUS expression patterns. As shown in Figure 2 and Supplementary Figure S2, the *DME* promoter lines showed strong GUS staining in all tissues analysed, including leaves, roots, flowers and siliques. No visible difference in GUS staining could be observed between the two versions of the *DME* promoter constructs, *DME+TEp*:GUS and *DMEp*:GUS. In addition, quantitative expression analysis of four independent lines for each of the *DME* constructs, using a fluorometric MUG assay, detected no significant difference in GUS expression levels between the two (Supplementary Figure S3). This indicated that the additional upstream TE sequence in *DME+TEp*:GUS is not required for *DME* expression. The GUS expression pattern of the two *DME* promoter constructs confirmed that *DME* is transcribed throughout the reproductive and vegetative tissues of Arabidopsis, which is consistent with the RT-PCR result of Ortega-Gallisteo et al. [6].

The *ROS1p*:GUS promoter construct showed a much lower expression than the *DMEp*:GUS promoter constructs and displayed distinct expression patterns in different tissues. The expression level was relatively high in young leaves, particularly in the midrib areas, and in young flowers and siliques, but weaker in roots and older leaves and siliques (Figure 2 and Supplementary Figure S2). This was consistent with the *ROS1* expression pattern recorded in the AtGenExpress and TraVa databases [10,11], which showed relatively high



Figure 2. Representative expression patterns of the promoter:GUS fusion transgenes in *Arabidopsis* Col-0 ecotype. Arrow indicates *DML3p:GUS* expression in anthers of young flowers.

levels in the shoot apex and flower tissues but low levels in root, stem and leaves (Supplementary Figure S1A).

The *DML2p:GUS* construct showed weak expression in leaves and roots, with clear GUS staining mainly in the leaf midrib areas. However, it was strongly expressed in the flowers and siliques (Figure 2 and Supplementary Figure S2). This result indicated that *DML2* is predominantly expressed in reproductive tissues.

The *DML3p:GUS* construct displayed the most tissue-specific expression pattern among the demethylase gene promoter constructs. The *DML3p:GUS* lines showed no detectable GUS staining in young seedlings, siliques or most flower tissues (Figure 2 and Supplementary Figure S2). However, clear GUS staining was consistently detected in young (but not old) anther tissues after an extended period of staining (up to three days), which matched the data recorded in the TraVa database [11]. Thus, *DML3* is likely to be an anther-specific demethylase gene.

RNA interference knockdown of *DME* in *rdd* increases plant susceptibility to *Fusarium oxysporum* infection

In order to examine if *DME* contributes to DNA demethylase function in somatic tissues, a hairpin RNA construct (hpDME) was designed to silence *DME* specifically in green tissues. We used the *Arabidopsis rubisco* small subunit gene promoter (SSU) to drive the expression of hpDME (Figure 1). The 548 bp sequence of the *DME* cDNA in the hpDME construct had two short (20 and 21 nt) stretches of sequence identity with *DML2* but showed no high nucleotide sequence similarities to *ROS1* and *DML3*. This construct was transformed into *rdd* plants to achieve *DME* knockdown in the triple demethylase mutant background. We also introduced the construct into Col-0 to obtain *DME* knockdown lines in the wild-type background. Transgenic lines containing the hpDME construct showed no phenotypic difference to the untransformed *rdd* or the wild-type Col-0 plants, and were fully fertile (data not shown). Two single-copy transgenic lines in the *rdd* background, *rdd*-HP5 and *rdd*-HP6, were self-fertilized to generate homozygous progeny populations and used for disease response, gene expression and DNA methylation analyses.

Two hpDME lines of the Col-0 background, Col-HP4 and Col-HP7, were also included. Northern blot analysis of the target *DME* mRNA showed that *rdd*-HP5 plants had little hpDME expression, hence only a slight reduction in *DME* mRNA level was observed (Figure 3 and Supplementary Figure S4). *rdd*-HP6 plants, on the other hand, showed a high level of hpDME expression and concomitant strong downregulation of *DME* mRNA. Similarly, Col-HP4 showed clear hpDME expression and *DME* downregulation, but Col-HP7 had little hpDME expression or *DME* downregulation (Supplementary Figure S4). It was notable that lower-molecular-weight *DME*-specific hybridizing signals were also detected on the northern blots, but the nature of these bands remained unclear.

Our previous study showed that *rdd* plants have increased susceptibility to the fungal pathogen *Fusarium oxysporum* compared to Col-0 [5,8], suggesting that DNA demethylases play a positive role in *Fusarium* resistance. To examine if *DME* contributes to disease resistance, the homozygous T3 and T4 generations of *rdd*-HP5 and *rdd*-HP6 transgenic lines were assayed for disease susceptibility to *Fusarium*, along with Col-0 and *rdd* plants as controls. As shown in Figure 4, the *rdd*-HP6 plants, with strong downregulation of *DME*, showed a significant increase in the chlorotic disease phenotype compared with the parental *rdd* line, whereas *rdd*-HP5 plants, with only slight downregulation of *DME*, displayed a disease response similar to *rdd*. Soil infections yielded comparable results for these lines (Supplementary Figure S5). The Col-HP4 or Col-HP7 lines showed no detectable increase in *Fusarium* disease phenotypes compared to the Col-0 plant (Supplementary Figure S6), suggesting that knockdown of *DME* expression alone is insufficient to affect plant response to *Fusarium* infection.

***DME* contributes to gene expression regulation and DNA demethylation of promoter TEs of defence-related genes**

Our previous study has identified a subset of plant defence-related genes that are regulated by DNA demethylases in *Arabidopsis*: they contain transposable element (TE) sequences in their promoters and show differential DNA methylation in

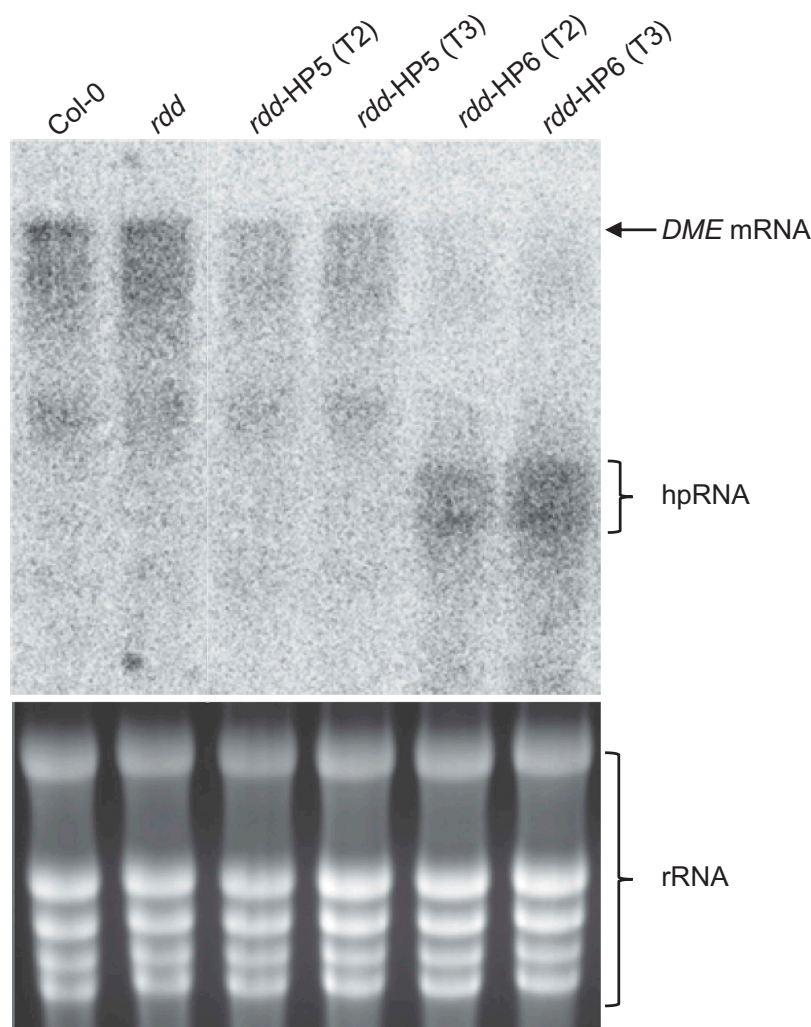


Figure 3. Northern blot analysis to detect *DME* mRNA level in Col-0, *rdd* and *rdd* *DME* RNAi transformants (*rdd*-HP5 and *rdd*-HP6). Top panel: Northern blot analysis probed with antisense *DME* RNA, which allows detection of both the *DME* mRNA and the hpDME-derived transcript. Bottom panel: Ethidium bromide-stained RNA agarose gel to show even loading of RNA.

the promoter TEs and repressed gene expression in *rdd* compared to Col-0 [5,8]. Among the three DNA demethylase genes, *ROS1* plays a dominant role, but *DML2* and *DML3* also function redundantly to regulate these genes [5]. To investigate if *DME* also contributes to defence gene regulation, we selected a number of these *rdd*-downregulated defence-related genes and compared their expression in Col-0, *rdd*, and hpDME lines in the *rdd* and Col-0 backgrounds.

As shown in Figure 5, these defence-related genes were downregulated in the *rdd* mutant compared to Col-0 plants, consistent with our previous findings [5,8]. RNAi-mediated knockdown of *DME* in Col-0 did not affect the expression of these genes (except for AT1G05700 which

appeared to show slight downregulation in the Col-0 *DME* RNAi lines), which was consistent with the *Fusarium* infection result (Figure S6). This suggested that downregulation of *DME* alone is insufficient, or the level of *DME* downregulation in this line is not high enough, to affect the expression of these genes or the disease responses. However, RNAi-mediated downregulation of *DME* in the *rdd* background clearly affected the expression of all six defence-related genes analysed, which showed increased repression compared to the parental *rdd* plants (Figure 5). Consistent with the greater *DME* knockdown in line *rdd*-HP6 compared to *rdd*-HP5, all analysed defence-related genes showed stronger downregulation in the *rdd*-HP6 line. This result

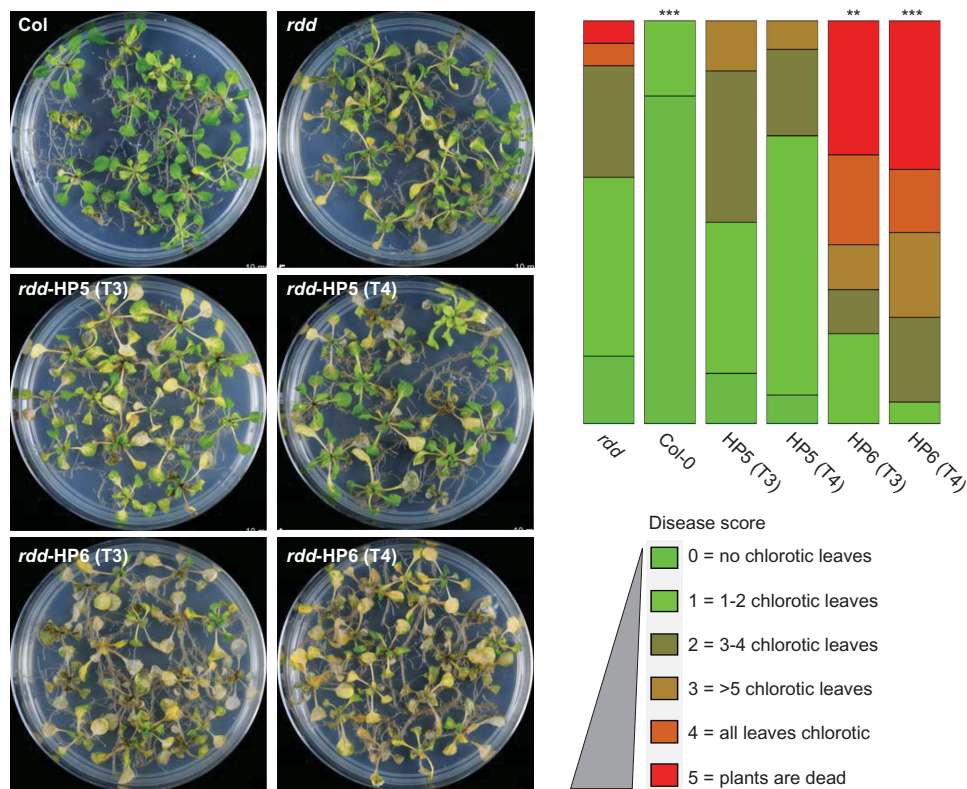


Figure 4. Knockdown of *DME* expression in *rdd* increases susceptibility to *Fusarium oxysporum* infection. Left panel: plants infected with *Fusarium* for 8 days at 23°C on sucrose-free MS medium. Right panel: histogram showing disease score based on the number of chlorotic leaves in each plant. Disease scoring was carried out in biological triplicates using 20–30 plants per replicate. The diagram was drawn using the software at <https://github.com/wangqinhu/aid>. Significance testing was performed using the Wilcoxon test: ** $p < 0.01$, *** $p < 0.001$.

indicates that *DME* contributes to the regulation of these defence-related genes.

Our previous studies have shown that the repressed expression of the defence-related genes in *rdd* were associated with differential DNA methylation at distinct loci coinciding with short TE sequences in the gene promoters, suggesting that *ROS1*, *DML2*, and *DML3* target the localized TE sequences to modulate DNA methylation levels and consequently gene expression [5,8]. To investigate if *DME* contributes to this demethylase function, we used bisulfite sequencing to determine the DNA methylation levels in the differentially methylated distinct promoter TE sequences of two *rdd*-downregulated defence-related genes that showed stronger repression in the *rdd* *DME* RNAi lines, AT3G27940 and AT4G33720. DNA samples of Col-0, *rdd*, *rdd*-HP5 (T3 generation), and *rdd*-HP6 (T3 and T4 generations) were isolated from 3 week old seedlings with no reproductive tissues and used for bisulfite conversion, as in the previous studies

[5,8]. Efficient bisulfite conversion of the DNA samples was confirmed by amplifying the chloroplast *psaA* gene sequence, known to be unmethylated, followed by digesting the PCR product with the *MseI* enzyme (Supplementary Figure S7). Consistent with our previous results, the *rdd* plants showed localized reduction of CHH methylation compared to Col-0 in the promoter TE sequences of both genes (Figure 6 and Supplementary Figure S8). The *rdd*-HP6 line, with strong downregulation of *DME*, showed a further reduction of CHH methylation levels in both gene promoter TE sequences compared to *rdd*. The *rdd*-HP5 line, with slight downregulation of *DME*, did not show a further reduction of CHH methylation in AT3G27940 (Figure 6) but displayed reduced CHH methylation in AT4G33720 compared to *rdd* (Supplementary Figure S8). The small number of CG sites (3 for AT3G27940 and 5 for AT4G33720) did not reveal a clear change in methylation level between the *rdd* *DME* RNAi lines and *rdd*, particularly as these

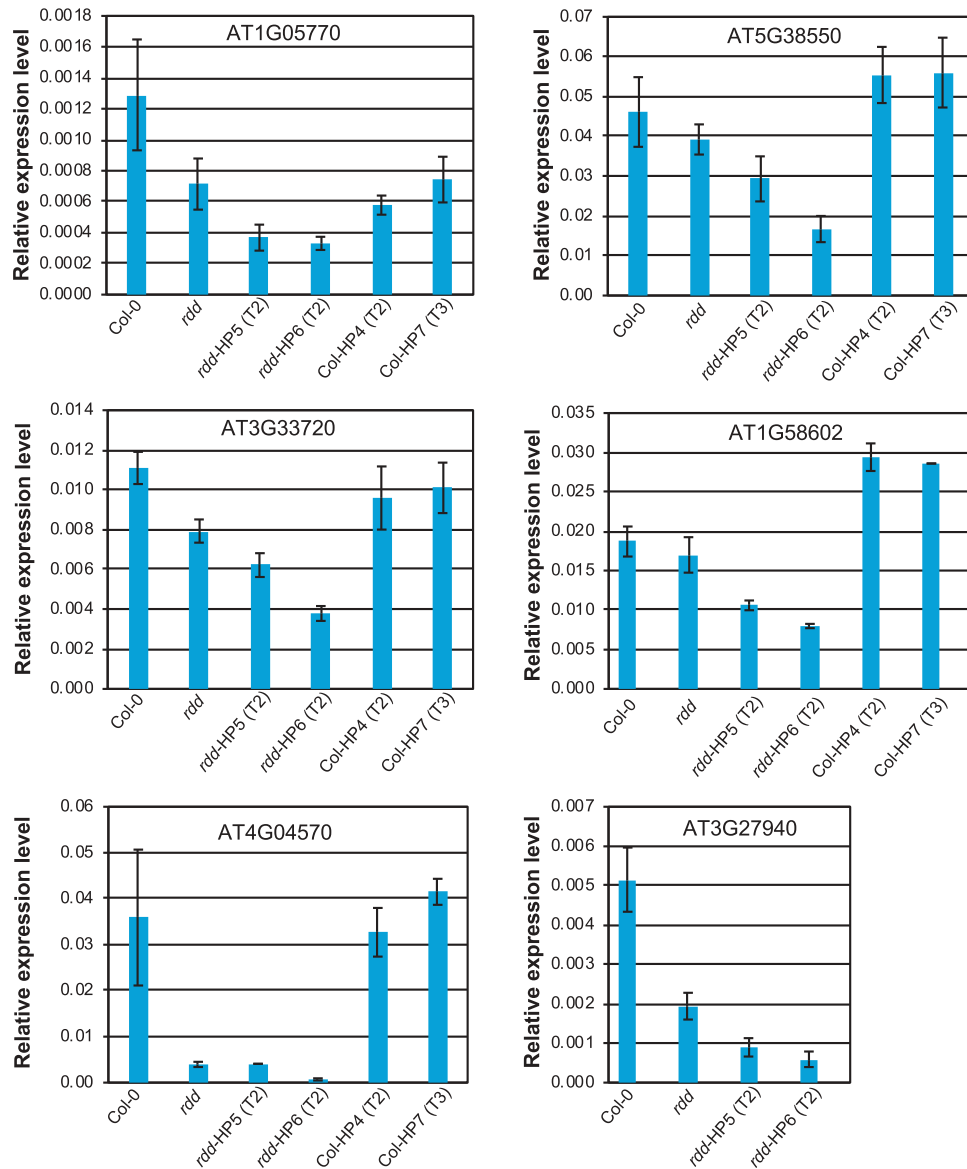


Figure 5. The expression levels of *rdd*-downregulated defence-related genes is further repressed by *DME* knockdown. Whole 3-week-old plants of around 20 individual siblings for each plant line were analysed as a pool. Columns indicate the average of three technical replicates with error bars showing standard deviation. The *Actin 2* gene was used as internal reference for RT-qPCR.

cytosines already showed almost complete methylation in *rdd* (data not shown [8]). Thus, the bisulfite sequencing analysis of the two promoter TE regions indicated that *DME* contributes to DNA demethylase function in the vegetative plant tissues.

Discussion

DME was initially thought to be expressed specifically in the central cell of female gametophytes, but subsequent gene expression studies by us and others suggested that *DME* is expressed constitutively in Arabidopsis. This prompted us to investigate if this

DNA demethylase gene might function together with *ROS1*, *DML2* and *DML3* in somatic tissues and contribute to DNA demethylation activity and plant defence response.

We first examined the expression pattern of *DME* as well as *ROS1*, *DML2*, and *DML3* using promoter:*GUS* fusion constructs. Our results confirmed the constitutive expression pattern of *DME*; the *DMEp:GUS* and *DME+TEp:GUS* constructs gave high levels of *GUS* expression across all tissues analysed. This result is consistent with the expression patterns recorded in AtGenExpress and TraVA [10,11].

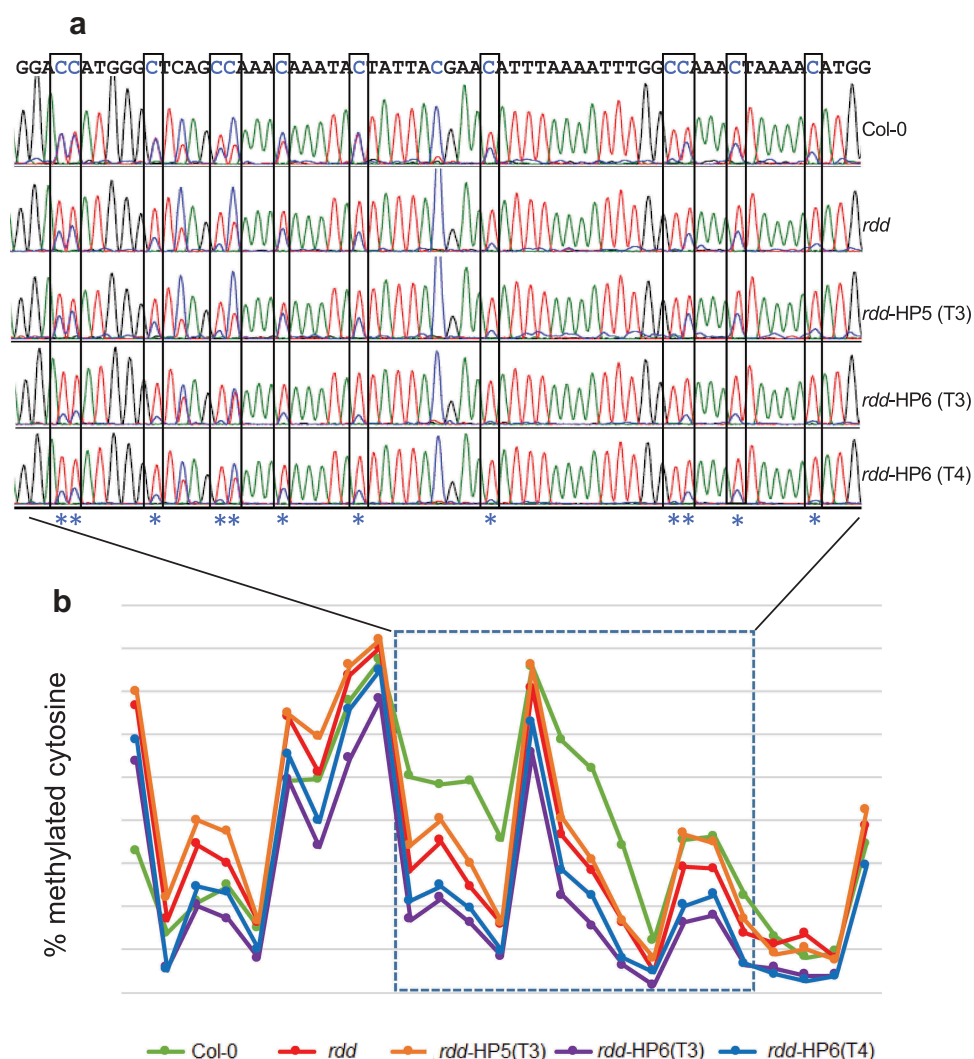


Figure 6. DME RNAi causes a further reduction in CHH methylation at the *rdd*-controlled promoter TE region of AT3G27940. a: Representative bisulfite sequencing trace file of the region showing CHH methylation changes. The CHH sites are boxed and indicated with asterisks. The ratio between blue and overlapping red peaks indicates the level of cytosine methylation. b: Cytosine methylation level of the whole bisulfite sequenced region. Each point represents one cytosine residue in the CHH context. The section for which the trace file image is shown is indicated.

However, the tissue-differential and tissue-specific expression patterns of *ROS1p:GUS*, *DML2p:GUS* and *DML3p:GUS* observed in this study, particularly of *DML2p:GUS* and *DML3p:GUS*, are different to the strong constitutive expression patterns observed by Gong et al. [9] and Ortega-Gallisteo et al. [6], who also used promoter:*GUS* fusion constructs to investigate gene expression. One possible explanation lies in the difference in construct configurations between the previous reports and the current study. In the *ROS1*, *DML2* and *DML3* promoter:*GUS* fusion constructs used by Gong et al. [9] and Ortega-Gallisteo et al. [6], the promoter:*GUS* expression

cassettes were inserted adjacent to a cauliflower mosaic virus 35S promoter that was used to drive the expression of the selectable marker gene in the plant transformation vectors pCAMBIA1380 and pCAMBIA1381. Consequently, the *ROS1*, *DML2* and *DML3* promoters were placed in close proximity to the 35S promoter, a configuration that is known to cause constitutive expression of otherwise tissue-specific endogenous gene promoters, presumably due to the strong enhancer activity of the 35S promoter (e.g., [14]). In this study, we aimed to avoid this enhancer effect by using a plant transformation vector without a strong constitutive promoter and by placing the DNA

demethylase gene promoters distal to the promoter driving the selective marker gene. Therefore, the expression patterns of *ROS1*, *DML2* and *DML3* promoter:GUS fusion constructs observed in this study are more likely to represent the endogenous gene expression patterns than those reported by Gong et al. and Ortega-Gallisteo et al. [6,9].

While the tissue-differential expression pattern of the *ROS1p:GUS* construct is consistent with the *ROS1* expression data recorded in the AtGenExpress and TraVA databases, it was surprising that the expression level of *ROS1p:GUS* (as assessed by GUS staining) was weaker than that of *DMEp:GUS* and *DME+TEp:GUS* (Figure 2). This was also in contrast to the expression profile obtained from our microarray and mRNAseq analyses (Figure S1). A recent study showed that the activity of the *ROS1* promoter depends on DNA methylation at a target sequence near the transcription start site [15]. It is possible that the level of DNA methylation in the transgenic *ROS1* promoter did not reach the level of the endogenous promoter resulting in comparatively lower levels of GUS expression. This is worth investigating in future studies.

Consistent with widespread *DME* expression in somatic tissues, our results showed that RNAi-mediated knockdown of *DME* expression in the *rdd* mutant background increased the disease susceptibility to *Fusarium* infection. Furthermore, a number of the defence-related genes shown previously to be repressed in the *rdd* mutant [8], showed even stronger repression in the *DME* RNAi plants. This suggested that *DME* functions together with *ROS1*, *DML2* and *DML3* to regulate the expression of these defence-related genes mediating *Fusarium* resistance in Arabidopsis. These defence-related genes contain TE sequences in their promoters, and these were shown to be the target for DNA demethylases in our previous studies [5,8]. Thus, while genome-wide DNA methylation and gene expression analysis of the *DME* RNAi lines is required to fully evaluate the function of *DME* in somatic tissues, our results confirmed that *DME* contributes to the function of DNA demethylases in the regulation of defence-related genes and disease response in vegetative plant tissues.

In general, CHH methylation was reduced in *rdd*, CG methylation increased, while CHG methylation showed no clear trend of change. Our analysis here revealed further enhanced differential CHH

methylation in the *DME* RNAi plants compared to their parental *rdd* plants. The function of CHH methylation in gene regulation is not fully understood. While DNA methylation at the promoters tends to repress gene expression, our previous studies showed that the reduced CHH methylation at promoter TEs in the DNA demethylase mutants often correlates with repressed gene expression [5,8]. In addition, increased expression of an *rdd*-regulated gene under *Fusarium oxysporum* infection showed increased CHH methylation at the promoter TE sequence [5]. These previous observations suggest that CHH methylation can be associated with increased gene expression. This phenomenon has also been described previously in maize, where CHH methylation at the upstream region of genes correlates positively with gene expression levels [16]. How CHH methylation positively affects gene expression remains unclear. A previous study has shown that transcriptional activation of an upstream TE can result in cryptic transcriptional initiation affecting the expression of the downstream gene [17]. It is possible that CHH methylation at such a TE sequence may play a role in silencing the TE to repress TE-initiated cryptic transcription, thereby maintaining active expression of downstream genes.

RNAi knockdown of *DME* in the wild-type Col-0 background did not cause increased disease response to *Fusarium oxysporum* infection or clear changes in defence gene expression. This result suggested that *DME* contributes to, but is not the dominant player, in the DNA demethylation of somatic tissues in Arabidopsis. This is consistent with *ROS1* being the dominant DNA demethylase in these tissues [5]. However, it cannot be ruled out that a more dominant role of *DME* exists in the whole plant due to the constitutive expression pattern, but the level of *DME* downregulation in the Col-hpDME transgenic line was not high enough to show a stronger disease response or gene expression change. It is also possible that the genes chosen here for expression and DNA methylation analysis were not the most suitable reporters for analysing *DME* function, and other specific defence genes, which are not strongly downregulated in the *rdd* mutant, may exist as direct targets of *DME*.

We chose to analyse six defence-related genes previously shown to be strongly downregulated in *rdd*,

namely AT1G05700 (LRR kinase), AT5G38550 (Mannose-binding lectin superfamily protein), AT3G33720 (Cystein-rich secretory protein, Antigen 5, PR1-related), AT1G58602 (LRR and NB-ARC domain containing disease resistance protein), AT4G04570 (Cystein-rich receptor-like kinase) and AT3G27940 (LOB-domain containing protein 26). LRR kinases, as well as Mannose-binding lectin proteins, are known receptors that are important in recognizing pathogen-associated molecular patterns and modulate gene expression in response to fungal infections. Cystein-rich receptor-like kinases, as well as pathogenesis-related (PR) proteins, are also known to be important in plant defence against pathogens. As such, each of these gene products is directly involved in the defence of *Arabidopsis* against fungal pathogens, which is consistent with our findings outlined here as well as previously. Hence, efficient and timely regulation of these genes could be paramount in ensuring plant survival under *Fusarium oxysporum* infection. Understanding the effect of DNA methylation and active DNA demethylation of short promoter TE sequences containing transcription regulatory elements holds the key to understanding the dynamics of gene transcription activation in response to fungal infection.

Our understanding of DNA demethylase gene function in *Arabidopsis* somatic tissues has so far been based mainly on genome-wide DNA methylation and gene expression analyses of the *rdd* triple mutant, which detected a relatively small number of genomic loci with differential DNA methylation and gene expression [4,12,13]. It will be interesting to examine the DNA methylation and gene expression profiles in the *rdd* *DME* RNAi lines, which could reveal more widespread changes in DNA methylation and gene expression than those observed in *rdd*. We anticipate that more functional roles of DNA demethylases in plants might emerge in the future.

Materials & methods

Preparation of the promoter:GUS fusion and *DME* hairpin constructs

Promoter:GUS fusion constructs

To create the promoter:GUS reporter gene fusion constructs, DNA sequences upstream of the ATG of each individual demethylase gene were amplified

using LongAmp Taq (NEB, #M0323S), cloned into pGEM-T Easy (Promega, #A1360) and sequenced. Primer sequences used for amplifying the promoter fragments are listed in Supplementary Table 1. The promoters were then removed from pGEM-T Easy using *Sma*I digestion and inserted into the binary vector pBI101 at the *Sma*I site in front of the pre-existing GUS coding sequence. The final vectors were confirmed by sequencing.

DME hairpin construct

Using the primers *DME*-forward and *DME*-reverse (Supplementary Table 1) a 548 bp fragment of the *DME* coding region was amplified, cloned into the pGEM-T Easy vector and sequenced. The *DME* fragment was excised by restriction digestion with *Xba*I-*Cla*I and cloned in an antisense orientation in the *Xba*I-*Cla*I multi-cloning site of the pKannibal vector [18]. The *DME* fragment in the same pGEM-T Easy plasmid was excised by restriction digestion with *Xho*I-*Kpn*I and cloned in a sense orientation in the corresponding sites of the pKannibal/*DME* antisense plasmid. The *DME* sense and antisense sequences are spaced by the PDK intron already present in the pKannibal vector. The 1.6 kb Rubisco small subunit promoter (SSU promoter) was excised from the pBC vector (Promega) using *Sac*I-*Sal*I digestion, and cloned into the *Sac*I-*Xho*I site upstream of the *DME* inverted-repeat in pKannibal, replacing the 35S promoter. The SSU-*DME* hpRNA expression cassette was released by restriction digestion with *Not*I and cloned into the *Not*I site of the binary vector pBART. The SSU promoter was positioned adjacent to the T-DNA Right Border sequence.

Plant transformation and analysis of transgenic plants

All plant expression constructs were transferred to the *Agrobacterium tumefaciens* strain GV3101 using tri-parental mating in the presence of *E. coli* strain RK2013 [19] or by electroporation. Plants were transformed by floral dipping using *Agrobacterium* as described previously [20] and transgenic seeds harvested. Transgenic progeny seeds from floral-dipped plants were screened by sterilizing seeds using bleach/HCl solution [21] and germinated on MS media containing

kanamycin (50 mg/L) and timentin (150 mg/L). Positive transgenic plants were self-fertilized to generate T2, T3, or T4 populations for further analysis. The presence of the constructs was confirmed by kanamycin resistance, PCR and northern blot analyses.

GUS expression analysis

Histochemical analysis of GUS expression was performed by incubating whole plants with 2 mM X-gluc (5-Bromo-4-chloro-3-indolyl- β -D-glucuronide) (Sigma, #B5285) at 37°C or room temperature followed by destaining with ethanol [22] and imaging using the Leica MZFLIII fluorescence dissector microscope. Quantitative analysis of GUS expression was carried out by MUG (4-methylumbelliferyl- β -D-glucuronide) (Sigma, #M9130) fluorometric assay as described previously [23] using pooled samples containing around 20 sibling plants (T4 generation) for each line.

Northern blot analysis and RT-qPCR

RNA was isolated from 3-week-old whole plant tissue (with no reproductive tissues) of approximately 20 individual siblings for each plant line using Trizol Reagent (Invitrogen, #15596026) according to manufacturer's instructions. Northern blot analysis was performed essentially as described previously using the same hybridization buffer [24]: 10 μ g of RNA was separated on a 1.3% formaldehyde agarose gel and the RNA fragments transferred to Hybond-N membrane (GE Healthcare Amersham, #RPN203N) by capillary transfer in 10 x SSC buffer overnight. After UV cross-linking the membrane was pre-hybridized at 55°C for 2–3 h, and then hybridized overnight with antisense RNA probe transcribed from the same pGEM-T Easy vector used to make the hpDME construct. The membrane was washed at 65°C with the phosphate-based buffers described in the Promega protocol used in [24] followed by 15-min RNase A treatment at room temperature in 2 x SSC buffer. The filter was exposed to a Phosphor Imager screen for visualization of hybridization bands.

For RT-qPCR analysis, 4 μ g of total RNA was treated with RNase-free DNase I (Ambion, #AM2222) at 37°C for 20 min, and purified by phenol-chloroform and chloroform extraction and sodium-acetate-ethanol precipitation. The RNA was then reverse transcribed into cDNA using Superscript III (Invitrogen, #18,080,093) and 50 pmol of oligo-dT₂₂ primer (22 thymines) in a 40 μ l reaction according to manufacturer's instructions. The reaction was diluted to 300 μ l with water and 5 μ l was used for each qPCR reaction. qPCR reactions were performed in technical triplicates on a Corbett 2000 Rotor-Gene real-time PCR machine (Corbett Research), using Fast SYBR Green Master Mix (Applied Biosystems, #4,385,610) according to the manufacturer's instruction. The Arabidopsis *Actin2* gene was used as the internal reference gene and relative expression determined using the comparative quantification method [25]. Primer sequences are listed in Supplementary Table 1.

DNA bisulfite sequencing

Approximately 2 μ g of DNA was bisulfite converted using the EpiTect Plus DNA Bisulfite Kit (Qiagen, #59,124) following the manufacturer's instruction, yielding 50 μ l of converted DNA solution. To check the efficiency of bisulphite conversion, PCR amplification was first performed on a 157-bp sequence of the chloroplast-encoded *psaA* gene. All bisulfite PCR reactions were performed using the following PCR cycles: 12 min at 94°C followed by 10 cycles of 1 min at 94°C, 2:30 min at 50°C, 1:30 min at 72°C, and 30 cycles with 1 min at 94°C, 1:30 min at 55°C, 1:30 min at 72°C, with a final extension of 10 min at 72°C. Primer sequences are listed in Supplementary Table 1. The PCR product of the *psaA* gene was digested with *MseI* restriction enzyme and separated on a 4% NuSieve agarose gel; full digestion at the two *MseI* sites created by C to T conversion indicates complete bisulfite conversion of the DNA (Supplementary Figure 7) [26].

Plant growth and Fusarium infection assays

Arabidopsis seeds were sown on MS agar plates [27] supplemented with 3% sucrose and kept for 3

days at 4°C, followed by germination and growth at 22°C in a 16 h/8 h light/dark cycle. Plantlets were transferred to fresh MS plates after one week.

Fusarium oxysporum f.sp. *conglutinans* strain 5176 (obtained from Dr Roger Shivas, Queensland Department of Primary Industries and Fisheries, Australia) was grown in Potato-Dextrose Broth (Sigma, #P6685) at 28°C and spores collected by centrifugation. A *Fusarium* spore solution of 2×10^6 spores/ml was prepared, and 3-week-old plants were infected by root dipping as described previously [8]. Infected plants were transferred either to MS agar without sucrose or to soil and the disease symptoms scored at the indicated time post-infection.

Acknowledgments

We thank Carl Davies for photography.

Author contribution

Conceived and designed the study: MBW, US, TM; Performed experiments: US, JL, NS, MBW; Analysed the data: US, JL, NS, CZ, MBW; Wrote the manuscript: MBW, US, NS, TM, ED.

Compliance

The work described herein was carried out in compliance with the Code of Conduct and the required Health and Safety Regulations.

Disclosure statement

No potential conflict of interest was reported by the authors.

ORCID

Ulrike Schumann  <http://orcid.org/0000-0002-2379-1226>

References

- [1] Zhu JK. Active DNA demethylation mediated by DNA glycosylases. *Annu Rev Genet.* 2009;43:143–166. PubMed PMID: 19659441; PubMed Central PMCID: PMC3137514.
- [2] Bauer MJ, Fischer RL. Genome demethylation and imprinting in the endosperm. *Curr Opin Plant Biol.* 2011 Apr;14(2):162–167. PubMed PMID: 21435940; PubMed Central PMCID: PMC3082360.
- [3] Choi Y, Gehring M, Johnson L, et al. DEMETER, a DNA glycosylase domain protein, is required for endosperm gene imprinting and seed viability in Arabidopsis. *Cell.* 2002 Jul 12;110(1):33–42. PubMed PMID: 12150995.
- [4] Penterman J, Zilberman D, Huh JH, et al. DNA demethylation in the Arabidopsis genome. *Proc Natl Acad Sci U S A.* 2007 Apr 17;104(16):6752–6757. PubMed PMID: 17409185; PubMed Central PMCID: PMC1847597.
- [5] Schumann U, Lee J, Kazan K, et al. DNA-demethylase regulated genes show methylation-independent spatio-temporal expression patterns. *Front Plant Sci.* 2017;8:1449. PubMed PMID: 28894455; PubMed Central PMCID: PMC5581395.
- [6] Ortega-Galisteo AP, Morales-Ruiz T, Ariza RR, et al. Arabidopsis DEMETER-LIKE proteins DML2 and DML3 are required for appropriate distribution of DNA methylation marks. *Plant Mol Biol.* 2008 Aug;67(6):671–681. PubMed PMID: 18493721.
- [7] Yu A, Lepere G, Jay F, et al. Dynamics and biological relevance of DNA demethylation in Arabidopsis anti-bacterial defense. *Proc Natl Acad Sci U S A.* 2013 Feb 5;110(6):2389–2394. PubMed PMID: 23335630; PubMed Central PMCID: PMC3568381.
- [8] Le TN, Schumann U, Smith NA, et al. DNA demethylases target promoter transposable elements to positively regulate stress responsive genes in Arabidopsis. *Genome Biol.* 2014;15(9):458. PubMed PMID: 25228471; PubMed Central PMCID: PMC4189188.
- [9] Gong Z, Morales-Ruiz T, Ariza RR, et al. ROS1, a repressor of transcriptional gene silencing in Arabidopsis, encodes a DNA glycosylase/lyase. *Cell.* 2002 Dec 13;111(6):803–814. PubMed PMID: 12526807.
- [10] Schmid M, Davison TS, Henz SR, et al. A gene expression map of Arabidopsis thaliana development. *Nat Genet.* 2005 May;37(5):501–506. PubMed PMID: 15806101.
- [11] Klepikova AV, Kasianov AS, Gerasimov ES, et al. A high resolution map of the Arabidopsis thaliana developmental transcriptome based on RNA-seq profiling. *Plant J.* 2016 Dec;88(6):1058–1070. PubMed PMID: 27549386.
- [12] Lister R, O'Malley RC, Tonti-Filippini J, et al. Highly integrated single-base resolution maps of the epigenome in Arabidopsis. *Cell.* 2008 May 2;133(3):523–536. PubMed PMID: 18423832; PubMed Central PMCID: PMC2723732.
- [13] Stroud H, Greenberg MV, Feng S, et al. Comprehensive analysis of silencing mutants reveals complex regulation of the Arabidopsis methylome. *Cell.* 2013 Jan 17;152(1–2):352–364. PubMed PMID: 23313553; PubMed Central PMCID: PMC3597350.
- [14] Zheng X, Deng W, Luo K, et al. The cauliflower mosaic virus (CaMV) 35S promoter sequence alters the level and patterns of activity of adjacent tissue- and organ-specific gene promoters. *Plant Cell Rep.* 2007 Aug;26(8):1195–1203. PubMed PMID: 17340093.
- [15] Lei M, Zhang H, Julian R, et al. Regulatory link between DNA methylation and active demethylation

- in Arabidopsis. *Proc Natl Acad Sci U S A*. 2015 Mar 17;112(11):3553–3557. PubMed PMID: 25733903; PubMed Central PMCID: PMC4371987.
- [16] Gent JI, Ellis NA, Guo L, et al. CHH islands: de novo DNA methylation in near-gene chromatin regulation in maize. *Genome Res*. 2013 Apr;23(4):628–637. PubMed PMID: 23269663; PubMed Central PMCID: PMC3613580.
- [17] Barkan A, Martienssen RA. Inactivation of maize transposon Mu suppresses a mutant phenotype by activating an outward-reading promoter near the end of Mu1. *Proc Natl Acad Sci U S A*. 1991 Apr 15;88(8):3502–3506. PubMed PMID: 1849660; PubMed Central PMCID: PMC51476.
- [18] Wesley SV, Helliwell CA, Smith NA, et al. Construct design for efficient, effective and high-throughput gene silencing in plants. *Plant J*. 2001 Sep;27(6):581–590. PubMed PMID: 11576441.
- [19] Ditta G, Stanfield S, Corbin D, et al. Broad host range DNA cloning system for gram-negative bacteria: construction of a gene bank of rhizobium meliloti. *Proc Natl Acad Sci U S A*. 1980 Dec;77(12):7347–7351. PubMed PMID: 7012838; PubMed Central PMCID: PMC350500.
- [20] Clough SJ, Bent AF. Floral dip: a simplified method for Agrobacterium-mediated transformation of Arabidopsis thaliana. *Plant J*. 1998 Dec;16(6):735–743. PubMed PMID: 10069079.
- [21] Wu Q, Smith NA, Zhang D, et al. Root-specific expression of a Jacalin Lectin family protein gene requires a transposable element sequence in the promoter. *Genes* (Basel) (Basel). 2018 Nov 13;9(11). DOI:10.3390/genes9110550. PubMed PMID: 30428604; PubMed Central PMCID: PMC6266147.
- [22] Jefferson RA, Kavanagh TA, Bevan MW. GUS fusions: beta-glucuronidase as a sensitive and versatile gene fusion marker in higher plants. *Embo J*. 1987 Dec 20;6(13):3901–3907. PubMed PMID: 3327686; PubMed Central PMCID: PMC553867.
- [23] Chen S, Helliwell CA, Wu LM, et al. A novel T-DNA vector design for selection of transgenic lines with simple transgene integration and stable transgene expression. *Funct Plant Biol*. 2005;32(8):671–681. PubMed PMID: WOS:000230931100001; English.
- [24] Wang MB, Wesley SV, Finnegan EJ, et al. Replicating satellite RNA induces sequence-specific DNA methylation and truncated transcripts in plants. *RNA*. 2001 Jan;7(1):16–28. PubMed PMID: 11214177; PubMed Central PMCID: PMC1370065.
- [25] Schmittgen TD, Livak KJ. Analyzing real-time PCR data by the comparative C(T) method. *Nat Protoc*. 2008;3(6): 1101–1108. PubMed PMID: 18546601.
- [26] Finn TE, Wang L, Smolilo D, et al. Transgene expression and transgene-induced silencing in diploid and autotetraploid Arabidopsis. *Genetics*. 2011 Feb;187(2):409–423. PubMed PMID: 21078688; PubMed Central PMCID: PMC3030486.
- [27] Murashige T, Skoog F. A revised medium for rapid growth and bio assays with tobacco tissue cultures. *Physiol Plantarum*. 1962;15(3):473–497. PubMed PMID: WOS:A19621781C00014; English.